Journal of Applied Mechanics and Technical Physics, Vol. 44, No. 5, pp. 648–653, 2003

STEADY STREAMWISE STRUCTURES IN THE BOUNDARY LAYER ON A SWEPT WING WITH ELEVATED TURBULENCE OF THE INCOMING FLOW

A. P. Brylyakov, G. M. Zharkova, B. Yu. Zanin, V. N. Kovrizhina, and D. S. Sboev

UDC 532.526

Results for a turbulized flow past the windward side of a swept wing model are presented. Origination of steady disturbances in the form of streamwise structures is found. The greatest effect on the formation of these disturbances is exerted by the curvature of the external flow streamlines. The secondary flow in the boundary layer leads to an increase in the characteristic scale of disturbances in the transverse direction, as compared to the flow around the model at a zero yaw angle.

Key words: *flow visualization, three-dimensional boundary layer, streamwise structures.*

Introduction. The problems of the turbulent flow around the wing are of interest both from the fundamental and applied viewpoints. Crossflow-conditioned effects play an important role in many engineering applications. The boundary layer under these conditions is one typical example of a three-dimensional boundary layer. Three-dimensional boundary layers are known to be susceptible to instability of several types. The most characteristic type is the instability of the secondary (transverse) flow [1]. It is this type of instability that plays the governing role in most cases at the initial sector of the swept wing at small angles of attack, because the Tollmien–Schlichting instability is suppressed by the favorable pressure gradient, and separation phenomena are rarely observed. Most frequently, the crossflow instability leads to the formation of a system of streamwise vortices near the leading edge, which are usually oriented along the streamlines of the external flow. Origination of these vortices can be associated with the action of surface roughness and external turbulence on the flow.

The influence of external turbulence on evolution of disturbances in a three-dimensional boundary layer was considered in detail in [2], where it was found that the most important mechanism is the generation of unsteady crossflow disturbances by external turbulence, whereas the excitation of steady vortices by spatial inhomogeneities of the incoming flow generated by turbulizing grids or by inhomogeneities with a wavelength of the order of the model thickness is rather weak. This conclusion is supported by the theoretical data of [3]. At the same time, it turned out that the overall level of turbulence of the incoming flow affects the steady modes. In particular, it follows from the results of [2] that the vortex amplitude in the initial section increases with increasing turbulence level, but the vortices themselves decay.

Along with the crossflow instability near the leading edge of a swept wing, other mechanisms caused by the strong curvature of streamlines in this region can excite disturbances in the boundary layer: the Görtler-type instability near the stagnation line of the flow [4] or the mechanism of extension and amplification of external flow vorticity on curved streamlines, which was first considered in [5]. The data of [4] on the Görtler instability of the flow near the front stagnation point were analyzed in [6], where it was demonstrated that this flow is stable to infinitesimal perturbations. The nonlinear theory [5], in turn, was supported by the experiments of [7].

Origination of steady streamwise vortex structures in two-dimensional boundary layers on the windward side of nonswept wings at high angles of attack and high external turbulence was registered in [8–10]. The results of these works show that origination of vortex structures is caused by the strong curvature of streamlines near the front stagnation point. The objective of the present work, which is a continuation of [8–10], is to study the effect of the yaw angle of the model on steady vortex disturbances.

Institute of Theoretical and Applied Mechanics, Siberian Division, Russian Academy of Sciences, Novosibirsk 630090. Translated from Prikladnaya Mekhanika i Tekhnicheskaya Fizika, Vol. 44, No. 5, pp. 55–62, September–October, 2003. Original article submitted November 28, 2002; revision submitted March 13, 2003.

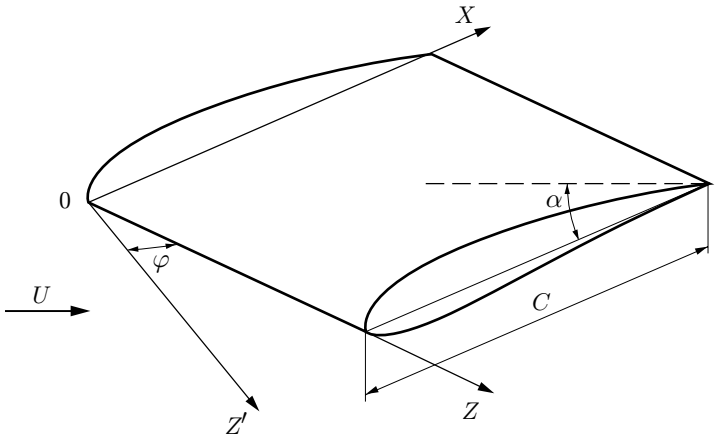

Fig. 1. Scheme of the model and coordinate system.

1. Test Conditions and Experimental Technique. The experiments were performed in an MT-324 wind tunnel of the Institute of Theoretical and Applied Mechanics of the Siberian Division of the Russian Academy of Sciences. This wind tunnel has an open test section and a square nozzle with an exit section of 200×200 mm. The free-stream turbulence is 0.4%. The research was performed both at this level of turbulence and at 1% turbulence reached by placing a turbulizing grid in the nozzle upstream of the test section. The grid was made of 0.3-mm wire with a cell size of 2.4 mm. The grid was located at a distance of 292 mm from the leading edge of the model, measured along the test-section centerline.

We studied the flow past the windward side of the wing model that had a symmetric profile with the maximum relative thickness equal to 16%, a chord $C = 228$ mm, and a span of 150 mm in the direction perpendicular to the incoming flow. Replaceable flat end washers of the wooden model were mounted to reduce the tip effects. The model could be positioned in the test section at different angles of attack α and yaw φ. The free-stream velocity was $U_\infty = 11.5$ m/sec. The Reynolds number based on the model chord was $\mathrm{Re}_C = 1.52 \cdot 10^5$. The following coordinate system was used in this work: the X axis was directed downstream perpendicular to the leading edge of the model and the Z axis was parallel to the latter; the origin was located on the leading edge (Fig. 1).

Visualization and measurement of the temperature field on the wing surface were performed by the method of liquid-crystal thermography [8–11]. The model surface was covered by a thin (20–25 μm) polymer–liquid-crystal film, which changed its color from red to blue with increasing temperature (within the range of selective reflection temperatures 31.0–35.5°C). During the experiments, the boundary conditions on the model surface necessary for visualization and temperature measurements were created by radiative heating, which provided satisfaction of the boundary condition of the second kind (constant heat-flux density). The color pattern on the model surface was registered by a videocamera. The initial signal was decomposed into the RGB scale (with basic colors are red, green, and blue) and fed into a computer. Then, the signal was transformed into the HIS (hue, intensity, and saturation) format more convenient for the subsequent analysis. The color distributions were recalculated into the temperature fields with the use of the calibration dependence of the hue on temperature, which ensured accuracy of 0.1°C. Videorecording with a rate of 25 frames per second yielded information on the temperature fields averaged within 40 msec. Interpretation of results is based on the fact that the temperature in regions with higher heat transfer is lower than that in regions with low heat transfer. The validity of this statement was verified in [10] by comparing the temperature fields and the mean velocity in the boundary layer measured by hot-wire anemometry.

2. Results. Figure 2 shows the distributions of the pressure coefficient $C_p = 2(P - P_\infty)/(\rho U_\infty^2)$ on the model in a highly turbulent flow. For $X/C \leqslant 0.2$ and $\alpha = 15$ and 27°, the negative pressure gradient is approximately identical. Further downstream, for $\alpha = 15°$, the favorable pressure gradient significantly decreases, and a small positive gradient is observed for $X/C > 0.5$. For $\alpha = 27°$, the pressure gradient is negative over the entire model surface, and its value in the region $X/C = 0.2$–0.5 is higher than for $\alpha = 15°$. The pressure distribution on the model mounted at zero incidence and flow visualization showed that a separation bubble was observed in this case at $X/C = 0.35$–0.50.

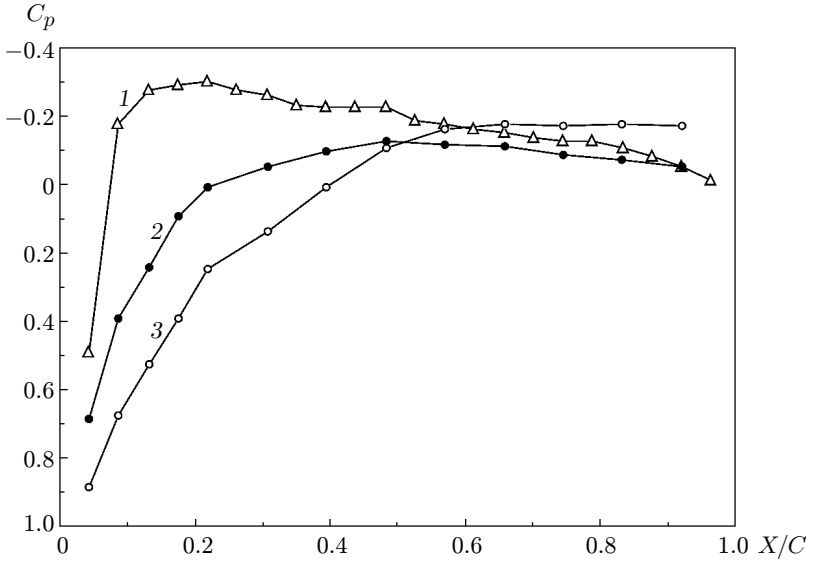

Fig. 2. Pressure distribution on the model surface in a highly turbulent flow ($\varphi = 15°$) for $\alpha = 0$ (1), 15 (2), and 27° (3).

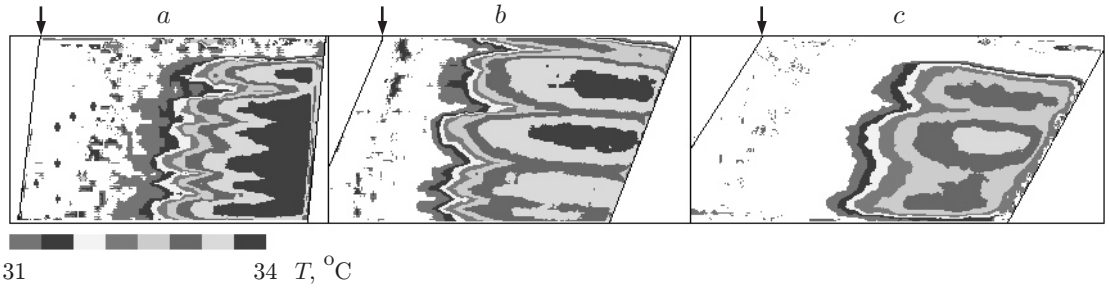

Fig. 3. Temperature fields on the windward surface of the model for $\alpha = 27°$ and $\varphi = 0$ (a), 15 (b), and 30° (c); the arrows indicate the position of the leading edge.

In visualization of the weakly turbulent flow around the model, the temperature fields on the model surface remained comparatively uniform (except for the corner regions) in the transverse direction for all examined combinations of the angles of attack and yaw, i.e., no streamwise structures typical of crossflow instability were observed in this case. This indicates that instability is weakly manifested here. It was shown in [12] on the basis of oil-film visualization of the flow on a swept cylinder that the streamwise structures appear if the crossflow Reynolds number is higher than 220, which requires higher values of U_∞ and φ than those used in our case. For instance, in [13], steady vortices arising due to crossflow instability on a swept cylinder 300 mm in diameter could be registered by the method of liquid-crystal thermography for $\varphi > 40°$ only; the incoming flow velocity was 40 m/sec. In the present work, we study regimes with $\varphi \leqslant 30°$, significantly lower values of U_∞ and rounding radius of the leading edge, and correspondingly, lower crossflow Reynolds numbers. Thus, in the low-turbulent flow around this model, crossflow instability has a weak effect on visualization patterns, which is in line with the results of the previous studies.

Figure 3 shows the wall-temperature fields for one variant of model mounting in a turbulized flow. Similar results were also obtained for other examined regimes. In contrast to the previously considered case of the low-turbulent flow, temperature modulation is observed here in the form of regions with elevated and reduced temperatures, which are localized in terms of the transverse coordinate and extended in the streamwise direction. Since heat transfer in an incompressible fluid is completely determined by the velocity field, we can state that there are streamwise structures in the flow around the model. A typical fact is that these structures are better visible on the rear part of the model. The streamwise structures are most clearly seen in experiments at high angles of attack.

It follows from Fig. 3 that the amplitude of temperature modulation increases downstream and reaches the stage of saturation. The wavelength remains constant along the transverse coordinate, and the structures are

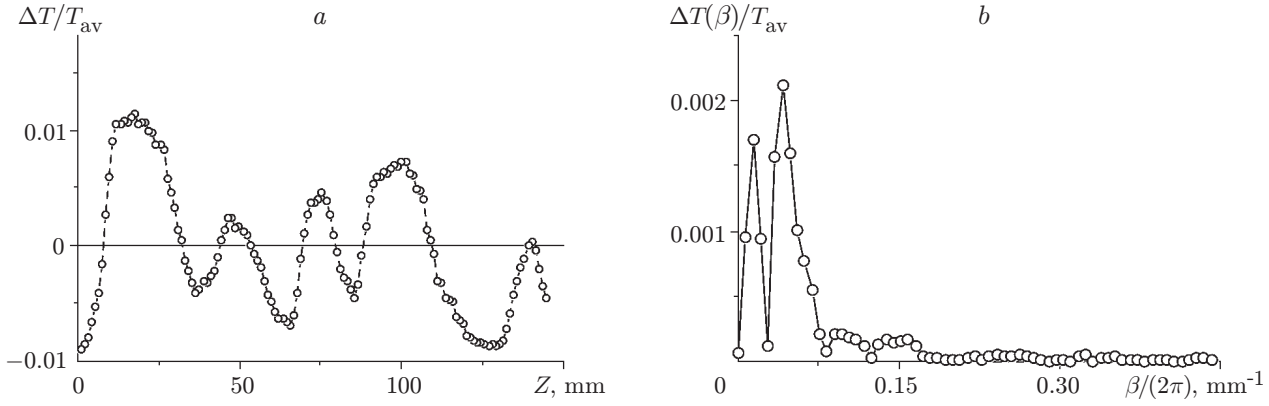

Fig. 4. (a) Distribution of wall-temperature variation for $\alpha = 15^\circ$, $\varphi = 15^\circ$, and $X/C = 0.5$; (b) the corresponding spectrum.

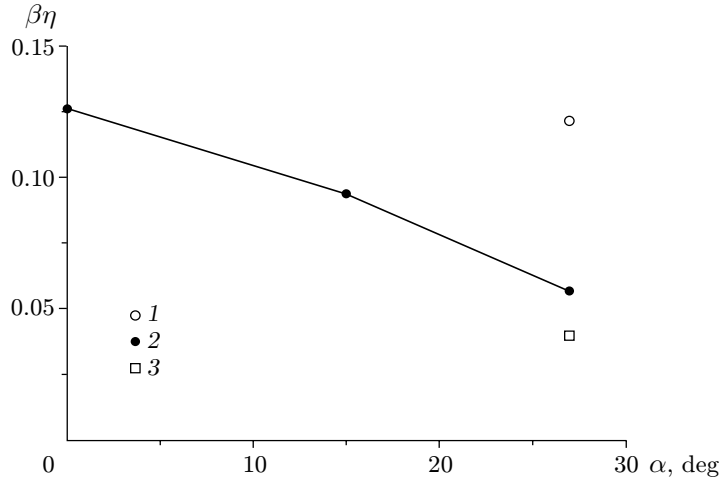

Fig. 5. Wavenumber versus the angle of attack for $\varphi = 0$ (1), 15 (2), and 27° (3).

oriented along the velocity vector of the external flow, which, in turn, is almost parallel to the velocity vector of the incoming flow due to the small span of the model and end washers. The wave amplitude and length depend on φ and α. With the help of digital processing of images, these disturbance characteristics can be correctly evaluated using the Fourier transform.

For one of the examined regimes, Fig. 4a shows the distribution of wall-temperature variation $\Delta T = T(Z) - T_{\text{av}}$ (T_{av} is the span-averaged temperature). Such a distribution is typical among those obtained in the present work. This distribution and similar ones were subjected to the Fourier transform over the transverse coordinate

$$\frac{\Delta T(\beta)}{T_{\text{av}}} = \frac{1}{T_{\text{av}} Z_0} \Big| \int_0^{Z_0} W(Z)\, \Delta T(Z) \exp\left(-i\beta Z\right) dZ \Big|^{1/2}.$$

Here β is the transverse wavenumber, $W(Z)$ is the weight function (Kaiser–Bessel "window"), and $Z_0 \approx 143$ mm is the record length (approximately constant in all cases). The spectrum corresponding to Fig. 4a is shown in Fig. 4b, where two peaks are visible. According to hot-wire measurements [10], the first peak (second harmonic with a period $Z_0/2$) arises due to Z-directed modulation of the mean-velocity field of the incoming flow in the test section of the MT-324 wind tunnel; the period of this modulation is 50–60 mm. The second peak (with a greater value) corresponds to streamwise structures arising in the boundary layer. Figures 5 and 6 show the wavenumber and amplitude corresponding to this peak as functions of α. The wavenumber is normalized to the self-similar coordinate $\eta = (\nu X/U_0)^{0.5}$ (ν is the kinematic viscosity and U_0 is the local mean velocity of the external flow, measured by a static pressure tube). The data were obtained in the region $X/C = 0.2$–0.5.

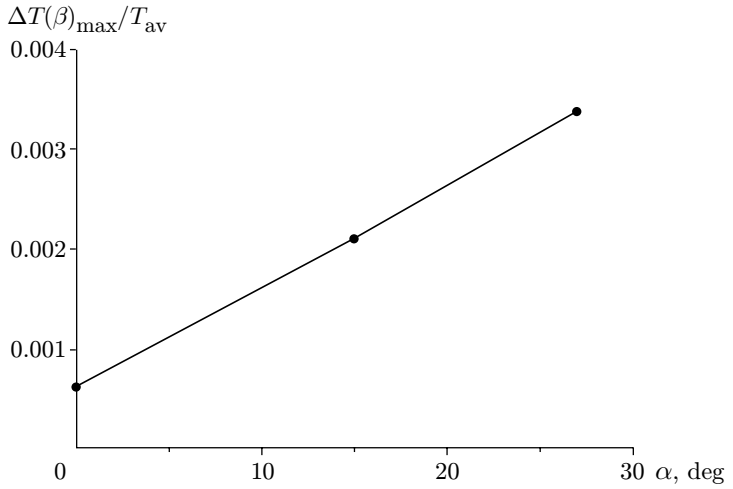

Fig. 6. Amplitude of wall-temperature variation versus the angle of attack for $\varphi = 15°$.

It follows from Fig. 5 that the dimensionless wavenumber decreases with increasing angle of attack at a constant φ, i.e., with increasing favorable pressure gradient (see Fig. 2). This contradicts the predictions of the linear stability theory for steady disturbances, according to which the thus-normalized wavenumber of the most unstable mode insignificantly increases with increasing favorable pressure gradient [14]. Moreover, the transverse wavelengths in this experiment were equal to 20–30 local boundary-layer thicknesses δ, which is much higher than (4–6)δ typical of unstable steady crossflow disturbances under "natural" conditions [2]. Nevertheless, these results are in qualitative agreement with the theory of vorticity extension and amplification [5], though this theory has been currently developed for two-dimensional flows only. The theory [5] predicts the existence of a neutral scale along the transverse coordinate, such that disturbances of smaller scale decay owing to viscous dissipation, and only disturbances whose scale is greater than the neutral value can be amplified. The neutral scale is of the order of several boundary-layer thicknesses and depends on the mean-flow properties, increasing (other conditions being equal) with increasing curvature of streamlines. Disturbances with scales greater than the neutral value are amplified more intensely. It should be noted that both dimensional and dimensionless wavelengths increase with increasing α for a constant φ. In particular, for $\varphi = 0$, similar results were obtained in [8, 9].

It follows from Fig. 5 that an increase in the yaw angle leads to an increase in the wavelength. The wavelength also increases in the coordinate system with the Z' axis perpendicular to the velocity vector of the incoming flow (see Fig. 1). This indicates the important role of the transverse flow in formation of streamwise structures, since the direction of external flow velocity on the rear part of the model (i.e., at a place where the streamwise structures are best visible) coincides with the incoming flow direction because of the small span of the model and the presence of end washers. In the model experiment [15, 16], the same effect caused by the influence of the secondary flow on the scale of disturbances generated by the action of a localized vortex from the external flow on the boundary layer was observed for low-frequency (quasi-steady) streamwise structures.

The amplitude of temperature fluctuations for a fixed value of φ increases with increasing angle of attack (see Fig. 6) and weakly depends on the yaw angle for large α. The increase in amplitude with increasing angle of attack is in qualitative agreement with the results of the theory of vorticity extension.

Thus, the results of the present study allow us to draw the following conclusions. Steady streamwise structure arise on the windward side of the swept wing under the present test conditions only if the model is exposed to a turbulized flow. The most effective generation is observed at high angles of attack, which is in agreement with results obtained previously for a nonswept wing. An important role in the formation of streamwise structures can belong to the mechanism of vorticity amplification on curved streamlines in the flow around the model. The effect of the secondary flow in the boundary layer is manifested in the increase in the characteristic scale of the structures along the transverse coordinate with increasing yaw angle of the model.

This work was supported by the Russian Foundation for Fundamental Research (Grant Nos. 01-01-00828 and 02-01-00006), Council on the grants of the President of the Russian Federation (Grant No. NSh-964.2003.1), and INTAS (Grant No. 00-00232).

REFERENCES

1. H. L. Reed and W. S. Saric, "Stability of three-dimensional boundary layers," *Annu. Rev. Fluid Mech.*, **21**, 235–284 (1989).
2. H. Deyhle and H. Bippes, "Disturbance growth in an unstable three-dimensional boundary layer and its dependence on environmental conditions," *J. Fluid Mech.*, **316**, 73–113 (1996).
3. M. V. Ustinov, "Receptivity of the boundary layer on a swept wing to steady inhomogeneity of the flow," *Izv. Ross. Akad. Nauk, Mekh. Zhidk. Gaza*, No. 3, 111–121 (2001).
4. J. Kestin and R. T. Wood, "On the stability of two-dimensional stagnation flow," *J. Fluid Mech.*, **44**, 461–479 (1970).
5. S. P. Sutera, P. F. Maeder, and J. Kestin, "On the sensitivity of heat transfer in the stagnation-point boundary layer to free-stream vorticity," *J. Fluid Mech.*, **16**, 497–520 (1963).
6. S. D. R. Wilson and J. Gladwell, "The stability of two-dimensional stagnation flow to three-dimensional disturbances," *J. Fluid Mech.*, **84**, Part 3, 517–527 (1978).
7. J. Bottcher and E. Wedemeyer, "The flow downstream of screens and its influence on the flow in the stagnation region of cylindrical bodies," *J. Fluid Mech.*, **204**, 501–522 (1989).
8. A. P. Brylyakov, V. N. Kovrizhina, B. Yu. Zanin, and G. M. Zharkova, "Spatial vortex system in the boundary layer over the windward side of wing," in: *Proc. of the 6th Asian Symp. on Visualization* (Pusan, May 27–31, 2001), BEXCO, Pusan (2001), pp. 269–271.
9. G. M. Zharkova, B. Yu. Zanin, V. N. Kovrizhina, et al., "Formation of a system of streamwise vortices on the windward side of the wing under elevated external turbulence," *Teplofiz. Aéromekh.*, **9**, No. 2, 213–215 (2002).
10. G. M. Zharkova, B. Yu. Zanin, V. N. Kovrizhina, and D. S. Sboev, "Steady streamwise vortices on a nonswept wing under elevated turbulence of the incoming flow," in: *Stability of Homogeneous and Heterogeneous Liquid Flows*, Abstracts of Int. Conf. (Novosibirsk, April 25–27, 2001), No. 8, Inst. Theor. Appl. Mech., Sib. Div., Russian Acad. of Sci., Novosibirsk (2001), pp. 67–68.
11. A. V. Dovgal', G. M. Zharkova, B. Yu. Zanin, and V. N. Kovrizhina, "Application of liquid-crystal coatings for studying flow separation," *Uch. Zap. TsAGI*, **32**, Nos. 3/4, 157–164 (2001).
12. D. I. A. Poll, "Some observations of the process on the windward face of a long yawed cylinder," *J. Fluid Mech.*, **150**, 329–356 (1985).
13. Y. P. Kohama, "Three-dimensional boundary layer transition study," *Current Sci.*, **79**, No. 6, 800–807 (2000).
14. L. M. Mack, "Boundary layer stability theory: Special course on stability and transition of laminar flow," AGARD Report No. 709, Paris (1984).
15. D. S. Sboev, G. R. Grek, and V. V. Kozlov, "Experimental study of receptivity of the boundary layer on a swept wing to localized disturbances from the external flow," *Teplofiz. Aéromekh.*, **7**, No. 4, 469–480 (2000).
16. A. V. Boiko, G. R. Grek, A. V. Dovgal, and V. V. Kozlov, *The Origin of Turbulence in Near-Wall Flows*, Springer-Verlag, Berlin (2002).